

27 Apr 1981, 2:00 pm - 5:00 pm

## Estimation of In-Situ Clay Strengths Using Marine Sediment Penetrators

R. L. McNeill

*Sandia National Laboratories, Albuquerque, NM*

A. D. Foster

*Sandia National Laboratories, Albuquerque, NM*

Follow this and additional works at: <https://scholarsmine.mst.edu/icrageesd>



Part of the [Geotechnical Engineering Commons](#)

---

### Recommended Citation

McNeill, R. L. and Foster, A. D., "Estimation of In-Situ Clay Strengths Using Marine Sediment Penetrators" (1981). *International Conferences on Recent Advances in Geotechnical Earthquake Engineering and Soil Dynamics*. 7.

<https://scholarsmine.mst.edu/icrageesd/01icrageesd/session01b/7>



This work is licensed under a [Creative Commons Attribution-Noncommercial-No Derivative Works 4.0 License](#).

This Article - Conference proceedings is brought to you for free and open access by Scholars' Mine. It has been accepted for inclusion in International Conferences on Recent Advances in Geotechnical Earthquake Engineering and Soil Dynamics by an authorized administrator of Scholars' Mine. This work is protected by U. S. Copyright Law. Unauthorized use including reproduction for redistribution requires the permission of the copyright holder. For more information, please contact [scholarsmine@mst.edu](mailto:scholarsmine@mst.edu).



# Estimation of In-Situ Clay Strengths Using Marine Sediment Penetrators

R. L. McNeill and A. D. Foster

Members of the Technical Staff, Sandia National Laboratories, Albuquerque, New Mexico

**SYNOPSIS** A method has been developed to calculate soil shear strengths from the measured decelerations of a free-fall penetrator. The method is easy to apply, and appears to yield accurate estimates of in-situ soil strength over a wide variety of soil conditions, and for many different sizes and weights of penetrators. For gassy and/or sensitive soils, the method may yield strength values more accurate than those determined by conventional boring, sampling, and laboratory testing.

## INTRODUCTION

A penetrator is a long, thin, pointed metal billet which impacts the earth and penetrates. Impact velocity is usually achieved by free-fall. Penetrators instrumented with accelerometers have demonstrated that the decelerations are a strong function of the strength of the soil being penetrated. For example, Figure 1 shows the deceleration record from a large penetrator impacting a soft clay overlying harder layered soils: the decelerations clearly are influenced by the relative strengths of the soils being penetrated. Thus, in principle,

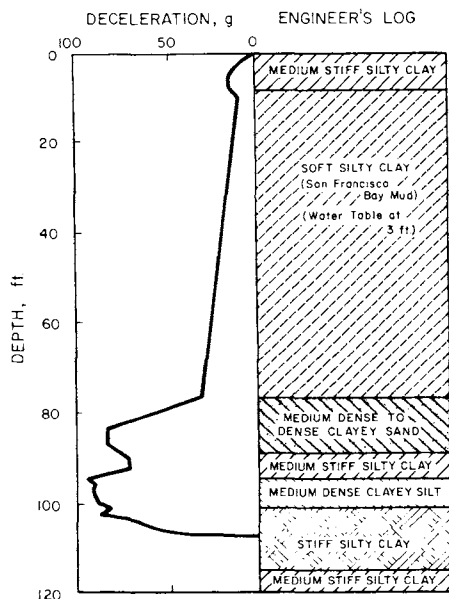


Fig. 1. Decelerations of Penetrator in Soils of Various Strengths

it should be possible to calculate soil strengths using the measured decelerations of a given penetrator impacting at a given velocity. This paper presents one approach to making such soil-strength calculations. The approach is guided

strongly by the experience of Sandia National Laboratories' program over the last twenty years, involving several hundred full-scale field experiments with instrumented penetrators, ranging in diameter from a few inches to 1-1/2 ft; weighing from a few tens to a few thousands of pounds; impacting at velocities from a few tens to a few thousands of feet per second into soils, rocks, ice, and permafrost, ranging in shear strength from a few tens to a few tens of thousands of pounds per square foot, and penetrating from a few inches to several hundred feet

This paper will deal mostly with the Marine Sediment Penetrator (MSP), developed by Sandia for rapid and inexpensive strength characterization of inaccessible and offshore sites.

## THE MSP SYSTEM

The MSP, shown in Figure 2, is a light, relatively portable unit specifically designed for marine use. It is long and thin, and is boat-tailed for hydrodynamic efficiency. The aft end is hollowed out to carry the instrument package.

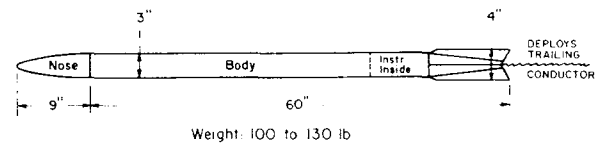


Fig. 2. Marine Sediment Penetrator, Model 2A

The prime instrument is an accelerometer, oriented longitudinally with the penetrator to measure the rigid-body axial forces (decelerations) experienced by the penetrator during its subterranean trajectory. The signals from the accelerometer are transmitted to the ship by an 0.1-in hard-wire conductor. The conductor is deployed from a special spool in the boat-tail section. The system in its simplest configuration deploys 650 ft of conductor; and, based on experience with the simple configuration, a system to deploy 3,000 ft has been designed.

For deeper waters, the penetrator is lowered to a predetermined distance above the seafloor to provide the required velocity at impact.

The penetrator can be launched in many ways. The simplest way is to drop it over the side of the ship. In this case, however, it takes about 400 to 500 ft to reach terminal velocity, which is 90 to 150 fps (depending on the weight of the penetrator). In soft clays such velocities will allow penetrations of about 30 to 50 ft. Thus for shallow waters or for deeper penetrations, the velocity must be augmented. This can be done by free-fall from an aircraft (both fixed-wing and helicopter have been used), but the accuracy is limited to within several hundred feet of a desired location. If better accuracy is required, the penetrator can be launched from a gun suspended over the side of the ship. Sandia has developed two types of guns: 1) a high-explosive recoilless (HER) gun; and 2) an air gun. The HER gun ejects a mass from its aft end for momentum equilibrium as the penetrator is launched from the other end; and that mass typically travels to great heights before descending at great velocities. The air gun requires a reaction weight or frame, or a recoil system.

Thus, there are several techniques available to achieve higher water-impact velocity, but these do not necessarily guarantee adequate seafloor-impact velocities. The penetrator starts to slow as it enters the water, and is at its terminal velocity (80 to 150 fps) at a depth of about 1,000 ft. Thus, for deep waters (>1,000 ft) and deep penetrations (>30-50 ft), the penetrator must be boosted underwater. It is for this reason that Sandia is presently developing an underwater launch-boost system.

TABLE 1. State-of-the-Art

Water Depth, Ft	Required Penetration, Ft	Method of Launch
100-400	20-30	Drop from ship
400-650	30-50	Drop from ship
650+	30-50	Lower, then drop
0-1,000	Unlimited	Underwater Gun (being developed) Air-drop, HER
1,000+	Unlimited	Underwater Gun (being developed)

Table 1 summarizes the present situations with respect to water and penetration depths achievable.

The basic data from a penetrator event is deceleration-time, an example of which is given in Figure 3. That record is integrated twice to obtain the impact velocity and final depth. The results are then cross-plotted to obtain deceleration-depth, as in Figure 4. The deceleration-depth format is the one used for calculations of soil strength, described in the next section.

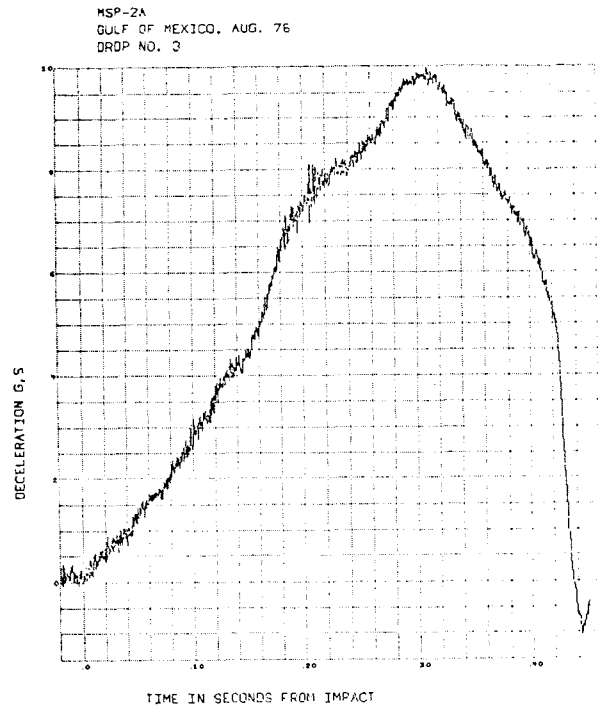


Fig. 3. Raw Data From Penetration Event

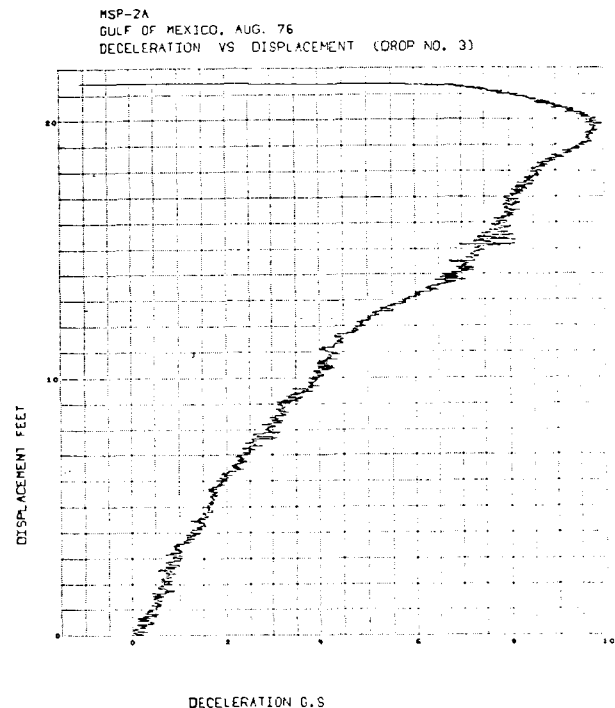


Fig. 4. Processed Data from Penetration Event

#### ANALYSIS OF PENETRATION EVENTS

As a penetrator moves through soil, its nose splits and shears the adjacent soil materials. Based on study of several hundred excavated penetrators impacting at low to moderate velocities (up to several hundred feet per second), the following are usually observed:

(1) the paint on the nose is gone, and often the metal is eroded; (2) the paint on the body is intact, or only lightly scratched, aft of the body's junction with the nose; (3) the paint on the aft section of the body is often gone; and (4) the radius of the final hole is less than the penetrator radius. Based on observation (1), it is hypothesized that the splitting action of the nose is very violent, and capable of imparting considerable lateral velocity to the adjacent soil particles. Based on (2), it is hypothesized that the lateral component of the imparted velocity is sufficient to make the hole larger than the penetrator, so that there is loss of contact between the soil and the penetrator. Based on (3) and (4), it is hypothesized that the hole may, under certain conditions, spring back into contact with the aft end of the penetrator before the penetrator has passed. Based on observations of the carefully excavated trajectories of several penetration events, it is further hypothesized that the penetrator moves down by shearing and pushing outward and upward an annulus of soil, to accommodate the penetrator's volume. Figure 5 has been prepared to show the general concept, and to define the dimensions which will be used in the formulations below.

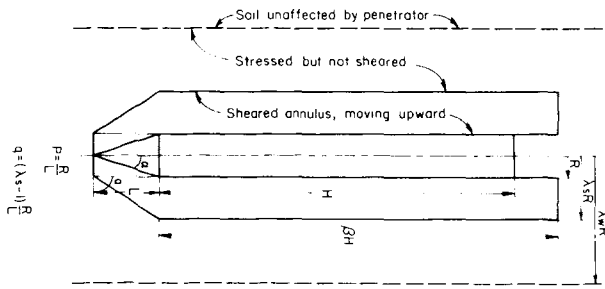


Fig. 5. Dimension Definitions

The radius of the sheared annulus of soil is taken to be some proportion,  $\lambda_s$ , of the penetrator radius,  $R$ ; and the length of the annulus is taken to be some proportion,  $\beta$ , of the body length,  $H$ . It is further hypothesized that, at some distance  $\lambda_w R$  from the penetrator, the soil is essentially unaffected by the penetration event. The soil between this unaffected zone and the sheared annulus is stressed, but likely not sheared to failure. Clearly, any analysis based on these concepts will depend on the choices of  $\lambda_s$ ,  $\lambda_w$ , and  $\beta$ , as will now be discussed.

The choice of  $\lambda_s$  has been considered analytically for piles by Beresantsev et al. (1961) who concluded that  $\lambda_s$  depends on the effective strength angle,  $\phi'$ , and would likely lie between about 2 and 4 for undrained shear. McNeill (1980a) empirically studied the appropriate value for  $\lambda_s$  using the results of many instrumented penetrator experiments to conclude that a value of  $\lambda_s = 2.6$  gave satisfactory results in most cases, comparing calculated strengths to measured strengths. That value,  $\lambda_s = 2.6$ , is used in all calculations in this paper.

The choice of  $\lambda_w$  has been studied for piles by Esrig et al. (1977), who used the theory of plasticity and material properties representative of soft clays to deduce that  $\lambda_w$  should be

about 20. That value,  $\lambda_w = 20$ , is used in all calculations in this paper.

The choice of  $\beta$  has been studied by McNeill (1980b), who derived an explicit expression for  $\beta$  based on the mechanism shown in Figure 6. In that mechanism, the impact of the nose generates a stress wave which propagates away from the penetrator. That wave travels through the sheared annulus and the stressed zone in Figure 5, but it encounters an acoustic-impedance boundary at the unaffected zone. The wave reflects from that boundary, and returns to the hole, to reflect from, and relieve the stress on, the particles of the hole. The hole then rebounds to a smaller size. If the penetrator is going rapidly, as in Figure 6(a), the rebound occurs after the penetrator has passed, and there is no soil attachment. If the penetrator is going slowly, Figure 6(b), the rebound will grasp the aft end of the penetrator,

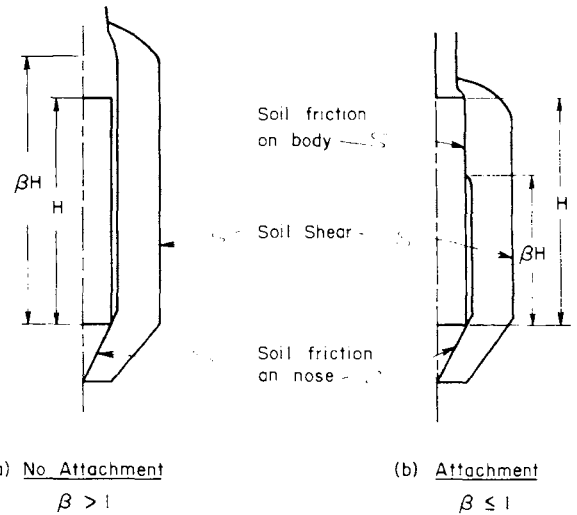


Fig. 6. Soil Attachment to Penetrator

slowing it further. Based on those considerations, the following expression for  $\beta$  was derived:

$$\beta = 2(\lambda_w - 1) \left( \frac{R}{H} \right) \left( \frac{\bar{v}_p}{\xi C_d} \right) \quad (1)$$

where  $\bar{v}_p$  is the average velocity of the penetrator at that point,  $C_d$  is the dilatational (seismic) velocity of the unstressed soil, and  $\xi$  is a factor by which that dilatational velocity is reduced because it is passing through a highly stressed zone. Anderson (1974) has studied the values of  $\xi$  for several clays. His results show that  $\xi$  varies from about 0.2 to perhaps 0.7, depending on stress level. The value of  $\xi = 0.35$  is used in all calculations in this paper. The final result is not strongly dependent on the choice of  $\xi$ .

Some of the important external stresses acting on the penetrator and on the soil annulus are shown in Figure 7(a,b).

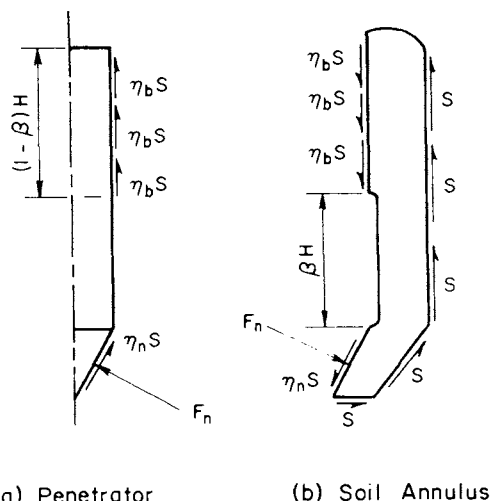


Fig. 7. Acting External Stresses  
(excluding inertia)

They consist of:  $\eta_b S$ , the skin friction acting on that part of the body and also on the soil annulus,  $(1-\beta)H$ , upon which soil attachment exists;  $\eta_n S$ , the skin friction acting on the nose and also on the soil annulus;  $F_n$ , the normal stress on the nose due to the splitting and transport of the soil annulus, and due to the shear strength,  $S$ , of the soil on the periphery of the annulus. Clearly, any analysis based on these concepts will depend on the choices of  $\eta_b$  and  $\eta_n$ , as will now be discussed.

Values of  $\eta$ , which is the ratio between the mobilized skin friction and the soil shear strength, have been addressed by Tomlinson (1969). He found that, for many types of driven piling in soft clays,  $\eta$  had values between 0.5 and 1. Because the penetrators used in the experiments to be described involved rapid shear (no consolidation), and because they were smooth and painted, the somewhat lower value of  $\eta_b = 0.3$  is used in all calculations in this paper. Because the paint, and sometimes some of the metal, are observed to be gone from the nose, it is reasoned that the stresses on the nose must be extremely high. For this reason, the value of  $\eta_n = 1.0$  is used in all calculations in this paper.

McNeill (1977, 1979) considered the external stresses depicted in Figure 7 to derive appropriate equations for calculating soil shear strength from the measured decelerations of a penetrator. The method gave good results when calculated strengths were compared to measured strengths, except for gassy or sensitive soils, where the calculated strengths agreed more with the conventionally measured strengths than with the known higher in-situ strengths. The differences were not large, but they existed. The approximations involved were: (1) the body friction,  $\eta_b S$ , was ignored; (2) some of the internal soil shears in the soil annulus near the nose were ignored; and (3) in the spirit of the approximation, the formulation of the inertia of the soil annulus did not completely take into account all the fundamental principles of mechanics. These approximations were addressed and substantially corrected by McNeill and Prindle (1980). It is the results of this latter, improved formulation which will now be

presented in this paper.

It is hypothesized that the important components of the total measured deceleration (force),  $D$ , acting on the penetrator are as follows: (1)  $D_t$ , the deceleration due to the inertia of splitting and transporting the soil away from the nose and up the annulus; (2)  $D_f$ , the deceleration caused by the attachment body friction,  $\eta_b S$ , if  $\beta < 1$ ; and (3)  $D_s$ , the deceleration caused by the shear strength,  $S$ , acting on the nose and the periphery of the upward-moving annulus. That is,

$$D_m = D_t + D_f + D_s \quad (2)$$

The derived expression for  $D_{t,n}$ , at a specific time,  $t_n$ , or depth,  $z_n$ , is:

$$D_{t,n} = C_1 \bar{V}_n^2 + C_2 \quad (3)$$

where

$$C_1 = \left( \frac{\gamma}{2gQ} \right) \left( \frac{\lambda_s^2}{(\lambda_s^2 - 1)^2} \right) \quad (3a)$$

$$C_2 = \left( \frac{\gamma}{Q} \right) (H + L) \quad (3b)$$

In the formulation,  $\gamma$  is the total unit weight of the soil,  $g$  is the acceleration of gravity,  $Q$  is the sectional pressure of the penetrator (total weight divided by frontal area), and all decelerations are in units of  $g$ . The derived expression for  $D_{f,n}$  is:

$$D_{f,n} = C_{f,n} S_n \quad (4)$$

where

$$C_{f,n} = \frac{2H\eta_b(1-\beta)}{QR} \quad (4a)$$

but:

$$C_{f,n} = \begin{cases} C_{f,n} & \text{for } \beta < 1 \\ 0 & \text{for } \beta \geq 1 \end{cases} \quad (4b)$$

The derived expression for  $D_{s,n}$  is:

$$D_{s,n} = (C_{s1,n} + C_{s2}) S_n \quad (5)$$

where

$$C_{s1,n} = \frac{2H\lambda_s}{QR(\lambda_s^2 - 1)} \beta_s \quad (5a)$$

but

$$\beta_s = \begin{cases} \beta & \text{for } \beta \geq 1 \\ 1 & \text{for } \beta < 1 \end{cases} \quad (5b)$$

$$C_{s2} = \frac{1}{Q} \left[ (1+\lambda_s)(1+\sin 2\alpha + q \cos 2\alpha) + \sin 2\alpha + \frac{\eta_n}{p \cos^2 \alpha} + p - 1 \right] \quad (5c)$$

It is important to note at this point that  $D_{f,n}$  (Eqn 4) and  $D_{s,n}$  (Eqn 5) both contain the soil shear strength  $S_n$  as a common factor. Solving these equations together results in an expression for the soil shear strength,

$$S_n = \left( \frac{1}{C_{s1,n} + C_{s2} + C_{f,n}} \right) (D_{f,n} + D_{s,n}) \quad (6)$$

The solution is obvious by recalling that  $D_m$  is a measured value, and  $D_{t,n}$  is calculated by Eqn (3), so that,

$$(D_{f,n} + D_{s,n}) = (D_{m,n} - D_{t,n}) \quad (7)$$

Thus,

$$S_n = \frac{1}{(C_{s1,n} + C_{s2} + C_{f,n})} (D_{m,n} - D_{t,n}) \quad (8)$$

It is helpful to recall the kinematic identity for calculating the average velocity,  $\bar{v}_n$ , to use in the calculation of  $D_{t,n}$ ,

$$\bar{v}_n = \frac{1}{2} \left[ \sqrt{v_{n-1}^2 - 2gD_{m,n}} + v_{n-1} \right] \quad (9)$$

where  $v_{n-1}$  is the velocity at the beginning of the 1-foot depth increment of the calculation.

In practice, the calculation of shear strength from deceleration proceeds as follows:

- (1) Double-integrate the raw deceleration-time data, Figure 3, to obtain the deceleration-depth curve, Figure 4. Divide the deceleration-depth curve into convenient increments (e.g., 1 ft), and select the value of  $D_{m,n}$  for each nth increment of depth.
- (2) Using  $D_{m,n}$  and Eqn (9), calculate the average velocity,  $\bar{v}_n$ , over that depth increment.
- (3) Estimate the soil density,  $\gamma$ , based on the general shape of the deceleration curve: if the curve indicates a soft material, select a low value, 90-100 pcf; if the curve indicates a hard material, select a high value, 130-140 pcf (this takes a little experience).
- (4) Estimate a value for  $\lambda_s$ . For the present, until ongoing theoretical and experimental studies shed more light on the matter, select  $\lambda_s \approx 2.6$ , for soft marine clays.
- (5) Using Eqn (3), calculate the value of the transport deceleration,  $D_{t,n}$ .
- (6) Estimate a value for  $\lambda_w$ . For the present, until ongoing theoretical and experimental studies shed more light on the matter, select  $\lambda_w \approx 20$ .
- (7) Estimate a value for  $\xi$ . Experience indicates that  $\xi$  should be at the lower end of the ranges identified by Anderson (1974). Select  $\xi \approx 0.2$  to 0.35.
- (8) Using the general nature of the deceleration depth curve (Figure 4), estimate the

dilatational velocity,  $C_d$  (this takes some experience, and it may be necessary to re-do the calculation with a better estimate of  $C_d$  based on the first calculation of the soil strength,  $S_n$ , referring to correlations of  $C_d$  or modulus of elasticity with strength.)

- (9) Using Eqn (1), calculate the value of  $\beta$ .
- (10) If  $\beta < 1$ , use Eqn (4a) to calculate the value of  $C_{f,n}$ . If  $\beta > 1$ , set  $C_{f,n} = 0$ , according to Eqn (4b).
- (11) Using Eqn (5a), calculate the value of  $C_{s1,n}$ . If  $\beta < 1$ , set  $\beta_s = 1$ , according to Eqn (5b).
- (12) Estimate a value for  $\eta_n$ . Lacking any other information, select  $\eta_n = 1$ .
- (13) Using Eqn (5c), calculate the value of  $C_{s2}$ . Note this value depends only on  $\lambda_s$  and the penetrator properties, so it is calculated only once.
- (14) Recall the measured  $D_{m,n}$  and the calculated  $D_{t,n}$  from step (5) above, apply Eqn (8) to calculate the soil shear strength,  $S_n$ , at that depth,  $Z_n$ .

The derivations of McNeill and Prindle (1980) do not take into account the boundary conditions at the ground surface, so that reliable calculated strengths should not be expected above a depth of one or so penetrator lengths. In some cases, the calculated value of shear strength,  $S$ , will be negative for the first few feet of calculation, because those surface boundary conditions are not properly accounted for. If the calculated strengths become positive at a depth of about half the penetrator length, then the calculated values of soil strength by about one or so penetrator lengths seem to agree well with measured values. If the calculated strengths do not become positive at a depth of about half a penetrator length, the value of  $\lambda_s$  should then be increased until the calculated strengths do become positive at about half a penetrator length.

The method is simple and quick to apply to calculate soil strengths. It is easily programmable for a computer, or for a hand calculator for field use. The next section will present some examples of application of the method.

#### SOME COMPARISONS TO MEASURED SOIL STRENGTHS

This section will present several comparisons of calculated to measured strength profiles, and will make the point that for certain conditions (e.g., gassy or sensitive soils), strengths calculated from penetrator data may be more representative of in-situ conditions than strengths measured by conventional techniques on samples raised through the water column to the surface. The examples are all for soft marine clays. The method has, however, been applied to very hard soils with similar results.

The first example is an experiment done at Vermillion, Block 301, in 196 ft of water. The

impact velocity was 78 fps, and the total penetration was 13 ft. A boring (Eustis Engineering) was available 600 ft away. The properties measured on the recovered samples were Atterberg limits, water contents, densities, shipboard miniature vane shear strengths, and laboratory unconfined compressive strengths. The Engineer's Log noted shell fragments and organic matter, but did not mention the presence of gas. Based on the measured densities and water contents, the recovered samples were all 100% saturated, so it is doubtful that gas was present. The data are shown in Figure 8. Also shown for reference are normal-consolidation (NC) strength lines for 0.2 and 0.3. It is clear that the measured strengths,

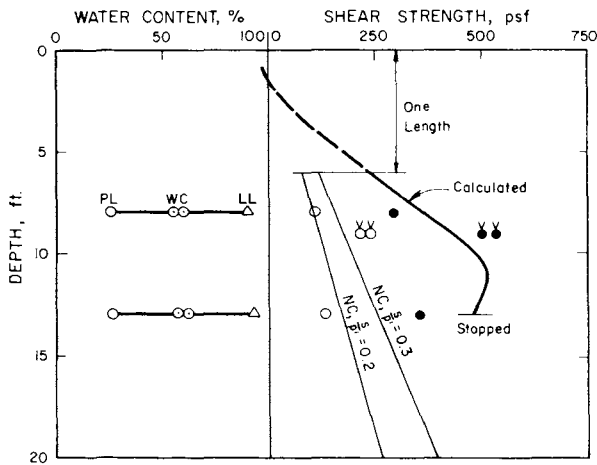


Fig. 8. Strength Comparisons (MSP-2A-2)

- Impact velocity = 78 fps
- Water depth = 196 ft
- Nonremolded
- o Remolded
- V Miniature shipboard vane, others unconfined

about 300 to 500 psf, exceed the predicted values for an NC clay. One is thus lead to characterize the soil as a non-gassy, slightly over-consolidated clay near the surface (8 ft), becoming weaker and less over-consolidated with depth (13 ft), and of moderate sensitivity (2-3).

The calculated shear strengths, using the method of the preceding section, are also shown in Figure 8. The calculated strengths below a penetrator length or so seem to reasonably represent the soil strength, lying within the band of the measured values, and showing the decrease with depth below about 11 ft.

The second example is an experiment done at South Pass, Block 48 in 238 ft of water. The impact velocity was 80 fps, and the total penetration was 21 ft. A boring (McClelland Engineers) was available 125 ft away. The properties measured on the recovered samples were Atterberg limits, water contents, densities, shipboard miniature vane shear strength, and Torvane shear strength. No Engineer's Log was available. The data are shown in Figure 9. The degrees of saturation, from 74% to 90%, indicate that the recovered samples must have had substantial gas in them at the time of testing

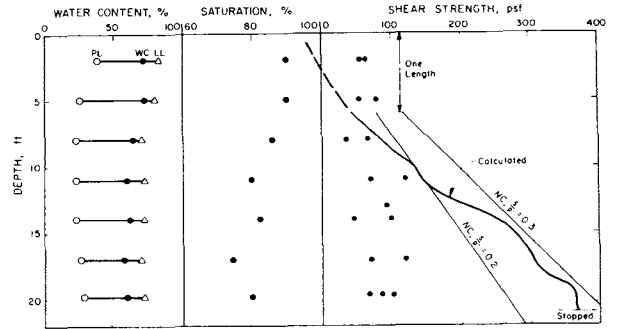


Fig. 9. Strength Comparisons, (MSP-2A-3)

- Impact Velocity = 80 fps
- Water Depth 238 ft
- Torvane and miniature vane, on shipboard (no remolded)

on shipboard. Esrig and Kirby (1977) have studied the effects of gasses, and predict that a shipboard saturation of 74% corresponds to an in-situ saturation (at 200 ft water depth) of about 95%; while a shipboard saturation of 90% corresponds to an in-situ saturation of about 98%. Thus, one would expect that the shipboard strengths are too low due to the disturbance from expansion of the gasses; and that the in-situ strengths must be higher but by an unknown amount. Noting the decrease in saturation with depth, Figure 9, one would also expect the discrepancy between the true and the measured strength to increase with depth. Inspection of the decrease in water contents and liquidity indices with depth would support this expectation, and would also suggest that the soil increases in degree of consolidation with depth.

All of these expectations are confirmed by the strengths calculated from the penetrator data, below about 1-1/2 penetrator lengths, Figure 9. In fact, the calculated strengths show the deposit to be an NC clay to the depths studied.

The foregoing example tends to indicate that for gassy soils, calculated strengths from penetrator data may be a more accurate representation of in-situ strengths than are shipboard or laboratory values. The same may be true for fragile soils which have liquidity indices greater than one, as the next example tends to indicate.

The third example is an experiment at South Pass, Block 70, in 390 ft of water. The impact velocity was 85 fps, and the total penetration was 29 ft. A boring was available (student cruise, Texas A&M University) 60 ft away. The properties measured on the recovered samples were Atterberg limits, water contents, and shipboard miniature vane shear strengths. No Engineer's Log was available. The data are shown in Figure 10. Because densities were not measured, the degrees of saturation cannot be calculated. There is available no other information on gas content. The liquidity indices are, however, rather high, which would lead to the expectation that the soil is underconsolidated, and perhaps sensitive. If the soil were sensitive, either of the following two situations would be expected:

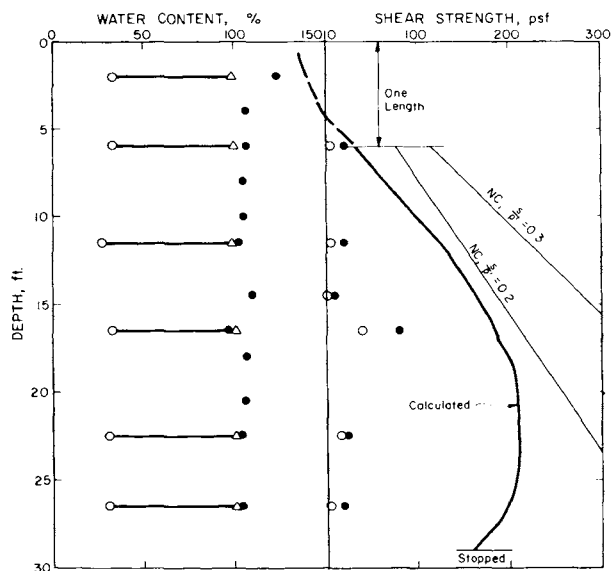


Fig. 10. Strength Comparisons (MSP-2A-6)

- Impact Velocity = 85 fps
- Water depth 390 ft
- Nonremolded, vane
- Remolded, vane

(1) if the sampling were of the very best quality, the remolded strengths should be much less than the nonremolded strengths (often referred to as "undisturbed" strength); or (2) if the sampling were not of the very best quality, the remolded strengths should not be very much different from the nonremolded strengths. The latter situation seems to apply here: as Figure 10 shows, the remolded and nonremolded strengths differ by little in most cases, and are equal in some cases.

The calculated shear strengths, Figure 10, indicate that the soil is underconsolidated, and that it was probably highly disturbed during the sampling process.

The preceding examples are for a specific penetration at several different sites. The next examples are for several different penetrators at the same site. The soils were deposited in a saline lacustrine terrestrial environment. The water table is presently a few inches below the surface, and the surface soils are desiccated to about 10 ft. The liquidity indices are high, Figure 11. Recognizing the possibility of high sensitivity, the samples were very carefully taken by pushing a thin-walled Shelby tube. The strengths were measured in the field by inserting a vane into the end of the sample tube, and in the laboratory by unconfined and triaxial (UU) compression. The results are given in Figure 12. As expected, the results show considerable scatter, but the bounded zone probably accurately represents the true variability of the site, considering the depositional environment. As a practical matter, the soils can be characterized as soft clay, increasing somewhat in strength with depth. Calculated strengths from penetrator data should show the same characterization.

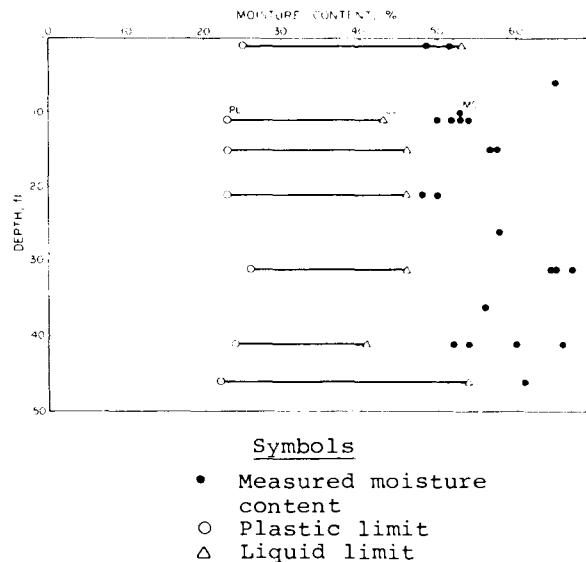
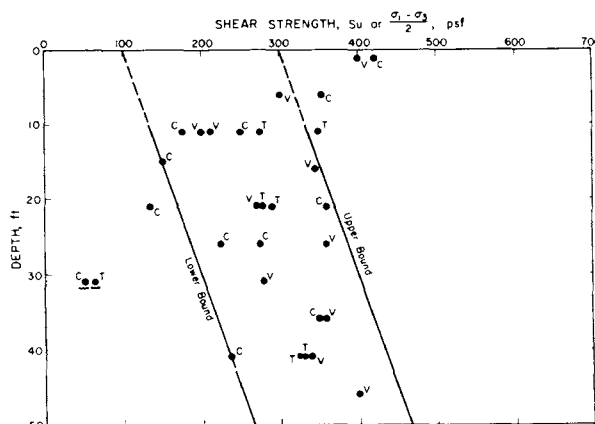


Fig. 11. Comparison of Natural Moisture Contents to Atterberg Limits



- Description of Symbols**
- V = Vane shear test, field (Torvane)
  - C = Compression test (unconfined)
  - T = Triaxial test (UU)
  - $\bar{C}, \bar{T}$  = Sample collapsed under self-weight.  $S_u$  assumed ~50 psf

Fig. 12. Measured Shear Strengths

The penetrators are shown to scale in Figure 13, along with their diameters, impact velocities ( $V_0$ ), and sectional pressures ( $Q$ ). The penetrators differ greatly in size (3 to 9 in. in diameter, 60 to 112 in. in length), weight (101 to 1500 lb), sectional pressure (14 to 25 psi), and impact velocity (133 to 242 fps). They all impacted within a 600-ft diameter circle, with the boring (Figure 12) near the center. Their measured average decelerations also varied considerably (I-9, ~10g; I-16, ~14g; II-3, ~5g; II-12, ~4g).



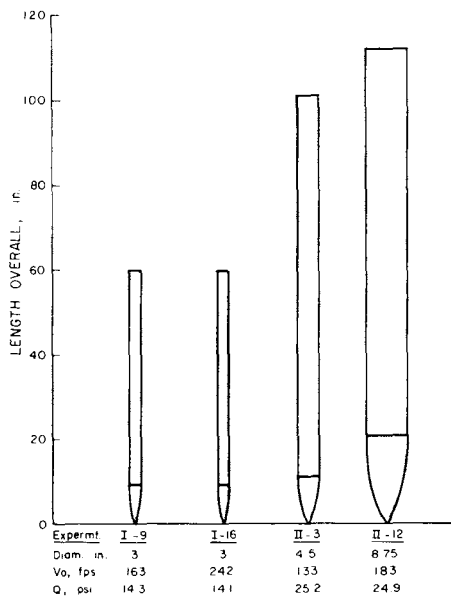


Fig. 13. Characteristics of Penetrators

Figure 14 shows the shear strengths calculated from the decelerations of these four different penetrators. The values seem to agree reasonably well with each other, and seem to be reasonably representative of the site's strength characteristics, at least within the variability of the strengths determined by conventional means.

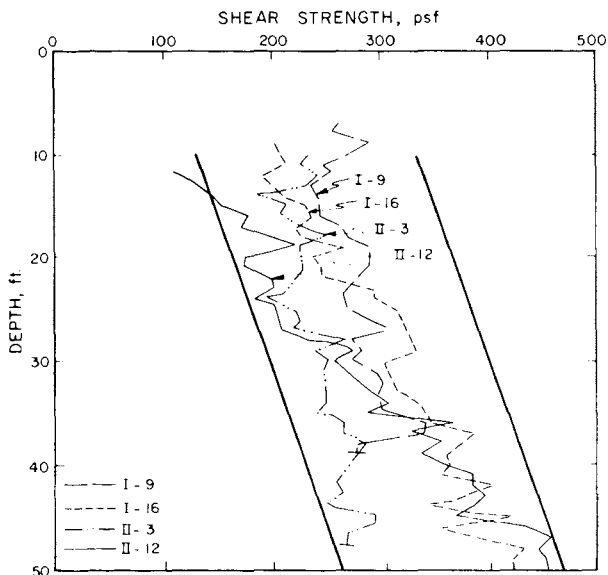


Fig. 14. Calculated Shear Strengths from Four Penetrators

#### CLOSURE

Instrumented penetrators have been used to calculate the strengths of marine soils, with good results when compared to conventionally measured strength values. When the calculated

and the measured values disagree, the calculated values appear to lie closer to what the in-situ values should be, considering what is presently known about the effects of gas and sensitivity disturbances.

The formulations are simple and easy to apply, and give good results over a wide range of soil conditions, and with a wide variety of penetrations.

#### ACKNOWLEDGEMENT

The data used here were obtained in experimental programs planned and executed by A. Foster, P. Wilkes, and C. W. Young, at Sandia National Laboratories. The figures were drawn by I. McNeill. The text was prepared by N. Gatchell.

#### REFERENCES

- Anderson, D. G. (1974), "Dynamic Modulus of Cohesive Soils", UMEE-74RZ, Univ. Mich., Ann Arbor.
- Beresantsev, Kristoforov, and Golubkov (1961), "Load Bearing Capacity and Deformation of Piled Foundations", Proc., 5th ICSMFE, Vol. 2, pp. 11-15.
- Esrig, M. I., and R. C. Kirby (1977), "Implications of Gas Content for Predicting the Stability of Submarine Slopes", Marine Geotechnology, Vol. 2, Lehigh Univ., Bethlehem, PA.
- Esrig, M. I., R. C. Kirby, R. G. Bea, and B. S. Murphy (1977), "Initial Development of a General Effective Stress Method for the Prediction of Axial Capacity for Driven Piling", Proc., OTC, Paper 2943.
- McNeill, R. L. (1977), "Preliminary Analysis of MSP1, MSP2, and MSP2A Penetration Events in Ocean-Bottom, Soft, Saturated Clays", Letter Report to M. Kramm, Dept. 1320, Sandia Laboratories, by R. L. McNeill, Consulting Engineer, Santa Ana, CA.
- McNeill, R. L. (1979), "Enhancement of Geophysical Soil Profiles Using Instrumented Marine Sediment Penetrators", Proc., OTC, Paper 3526.
- McNeill, R. L. (1980a), "Geotechnical Analysis of Penetrator Data, Wendover, UT", SAND80-2666C, Sandia National Laboratories, Albuquerque, NM.
- McNeill, R. L. (1980b), "An Approach for Estimating Soil Attachment during Penetration Events", SAND80-2667C, Sandia National Laboratories, Albuquerque, NM.
- McNeill, R. L., and R. W. Prindle (1980), "Derivation of Penetrator Equations", SAND80-2668C, Sandia National Laboratories, Albuquerque, NM.
- Tomlinson, M. J. (1969), "Foundation Design and Construction", Wiley, NY.